Synthesis and evaluation of *Strychnos* alkaloids as MDR reversal agents for cancer cell eradication

Surendrachary Munagala [a], Gopal Sirasani [a], Praveen Kokkonda [a], Manali Phadke [b], Natalia Krynetskaia [b], Peihua Lu [c], Frances J. Sharom [c], Sidhartha Chaudhury [d], Mohamed Diwan M. Abdulhameed [d], Gregory Tawa [d], Anders Wallqvist [d], Rogelio Martinez [b], Wayne Childers [b], Magid Abou-Gharbia [b], Evgeny Krynetskiy [b], Rodrigo B. Andrade [a,*]

[a] *Department of Chemistry, Temple University, Philadelphia, PA 19122, United States*
[b] *Department of Pharmaceutical Sciences, Temple University School of Pharmacy, Philadelphia, PA 19122, United States*
[c] *Department of Molecular and Cellular Biology, University of Guelph, Guelph, Ontario N1G 2W1, Canada*
[d] *Department of Defense Biotechnology High Performance Computing Software Applications Institute, Telemedicine and Advanced Technology Research Center, U.S. Army Medical Research and Materiel Command, Fort Detrick, MD 21702, United States*

ARTICLE INFO

ABSTRACT

Natural products represent the fourth generation of multidrug resistance (MDR) reversal agents that resensitize MDR cancer cells overexpressing P-glycoprotein (Pgp) to cytotoxic agents. We have developed an effective synthetic route to prepare various *Strychnos* alkaloids and their derivatives. Molecular modeling of these alkaloids docked to a homology model of Pgp was employed to optimize ligand–protein interactions and design analogues with increased affinity to Pgp. Moreover, the compounds were evaluated for their (1) binding affinity to Pgp by fluorescence quenching, and (2) MDR reversal activity using a panel of in vitro and cell-based assays and compared to verapamil, a known inhibitor of Pgp activity. Compound **7** revealed the highest affinity to Pgp of all *Strychnos* congeners ($K_d = 4.4$ μM), the strongest inhibition of Pgp ATPase activity, and the strongest MDR reversal effect in two Pgp-expressing cell lines. Altogether, our findings suggest the clinical potential of these synthesized compounds as viable Pgp modulators justifies further investigation.

© 2013 Elsevier Ltd. All rights reserved.

1. Introduction

Cancer is one of the leading causes of death worldwide, with multidrug resistance (MDR) being responsible for the failure of chemotherapy in >90% of metastatic cancer patients.[1] MDR is often characterized by the overexpression of ATP-dependent transporters, particularly P-glycoprotein (Pgp), which efflux anti-cancer drugs (e.g., taxol, vincristine, and doxorubicin) out of cancer cells.[2] In 1981, Tsuruo demonstrated that verapamil, a calcium-channel blocker, resensitized MDR cancer cells to vincristine.[3] It was later established that verapamil inhibits Pgp activity by direct competition with Pgp substrates.[4] While attempts to resensitize patient tumors to chemotherapy via MDR reversal (i.e., Pgp inhibition) have been largely unsuccessful to date in clinical trials, the accelerated discovery of natural product Pgp inhibitors (i.e., fourth generation) has reenergized the field.[5]

Within a decade of Tsuruo's discovery, clinical trials with first generation Pgp inhibitors (e.g., cyclosporine, verapamil, quinine)

were launched with optimism, as these drugs were already FDA-approved.[6] It was realized that the dosage required to inhibit Pgp was toxic to the patients; however, randomized Phase III clinical trials of cytarabine and daunorubicin in combination with cyclosporine in patients with poor-risk AML was beneficial.[7] In addition, the use of quinine in combination with chemotherapy showed an increase in complete remission rates and patient survival in Pgp-positive MDS cases.[8] The low affinity for Pgp was addressed to some extent with second generation inhibitors (e.g., valspodar, biricodar), but problems associated with pharmacokinetic interactions (i.e., metabolism and drug clearance due to cytochrome P450 inhibition) were responsible for failure in clinical trials. The third generation of Pgp inhibitors such as tariquidar, which were completely synthetic in origin and obtained through methodical combinatorial chemistry, possessed both nanomolar affinity for Pgp and optimal pharmacokinetic parameters. To date, the limited clinical studies of tariquidar have not conclusively shown MDR reversal. Bates has argued that negative results from clinical trials with Pgp inhibitors can be traced to poor clinical study design, particularly in patient selection, dosing regimen, and combinations thereof.[9] There is considerable interest in the development of

---

fourth generation inhibitors, which are largely natural product based. This is not surprising considering first-generation Pgp inhibitors cyclosporine and quinine, which yielded successful results in pioneering clinical trials, are, in fact, natural products.

Semi-synthetic derivatives of natural products provide a promising expansion of the oncologist's armamentarium, with 79% of all FDA-approved antineoplastic drugs derived from natural products.[10] To explore the potential of natural alkaloids and their semi-synthetic derivatives to reverse Pgp-mediated MDR, we have synthesized and evaluated various *Strychnos* alkaloids and analogues **1–7** for their capacity to bind Pgp and reverse MDR by (a) measuring binding affinity to Pgp by fluorescence quenching; (b) assessing the inhibitory effect of synthesized compounds on Pgp-associated ATPase activity, and (c) performing cell-based assays in two Pgp-overexpressing cell lines. Based on the structure of the natural compound leuconicine A, we have employed molecular modeling (i.e., docking studies) to maximize ligand-Pgp binding.

Kam and co-workers showed the MDR-inhibiting properties of structurally novel hexacyclic *Strychnos* alkaloids (−)-leuconicine A (**5**) and B (**6**), which were isolated from the Malaysian plant *Leuconotis maingayi*.[11] Prior to Kam's disclosure, we had developed a novel bis-cyclization method for preparing the tetracyclic core of the *Strychnos* alkaloids, and shortly thereafter applied this method toward the racemic syntheses of akuammicine (**1**) and strychnine.[12] Inspired by the architectural complexity of the leuconicines coupled with their MDR-reversing properties, we initiated a synthetic campaign to prepare these and related analogues to evaluate bioactivity (Fig. 1).[13]

Our method allows facile, efficient access to milligram quantities of analogues of these and other *Strychnos* alkaloids, in addition to the ability to test intermediates *en route* to the targets. We further expanded our approach by performing the first asymmetric syntheses of leuconicines A (**5**) and B (**6**). Herein, we describe the application of this strategy toward the syntheses of classic alkaloids (−)-akuammicine (**1**), (−)-dihydroakuammicine (**2**), (−)-norfluorocurarine (**3**), in addition to preparing analogues (−)-dehydroleuconicine B (**4**) and (−)-3,4,5-trimethoxybenzyl leuconicine A (**7**). Next, we evaluated the Pgp-binding properties of synthesized alkaloids, along with their potential to reverse Pgp-mediated MDR using a panel of in vitro and cell-based assays. In all evaluation studies we used verapamil as our standard Pgp competitive inhibitor.[14]

2. Results and discussion

2.1. Molecular modeling

A number of pharmacophores have been associated with affinity for Pgp.[15] We required a structural tool that would allow us to identify and design molecules with increased affinity to Pgp within the *Strychnos* alkaloid scaffold. To that end, we built a docking model of human Pgp (Fig. 2A). We carried out a BLAST search of the human Pgp sequence against the Protein Data Bank[16] and identified the protein structure of the mouse Pgp homolog,[17] with 86% sequence similarity, as a suitable template for homology modeling. We selected the mouse Pgp structure co-crystallized with the Pgp inhibitor QZ59-RRR (PDB code: 3G60, Fig. 2D) as a template and carried out homology modeling using Schrödinger's PRIME software,[18] followed by energy minimization and refinement using the default protocols in the software. We used Schrödinger's Glide software[19,20] for docking grid generation and ligand docking. The homology model was prepare for docking using the software's Protein Preparation Wizard tool. We generated a docking grid based on residues identified from structural and biochemical studies to be important for Pgp substrate binding.[12,21] Ligands were prepared using the Schrodinger Glide 'Ligprep' tool to sample all possible tautomers and all possible ionic states from a pH of 5.0 to 9.0. The three highest scoring poses were stored for each ligand. Docking was carried out using Schrodinger Glide's XS docking protocol. Two cyclic peptide inhibitors (QZ59-SSS and QZ59-RRR) that were previously co-crystallized with mouse Pgp (Aller et al. Science 2009) were re-docked into the human Pgp model to validate that the overall docking protocol recapitulated known ligand poses for this receptor.

Preliminary docking results revealed that many of the top ranking compounds docked to an aromatic-rich hydrophobic pocket formed by residues F72, F728, F732, V982, and F978 (dubbed 'site-1' by Ding et al.[21]), which is shown in Figure 2. Further analysis of the docked poses was necessary to elucidate the scaffold-specificity of various binding-site regions in Pgp and identify further analogues for synthesis possessing substituents that maximize binding affinity for a given scaffold class. Significantly, the best docking score was obtained with the third-generation MDR reversal agent tariquidar (score = −9.53), which is the most potent Pgp inhibitor developed to date. The modeling also predicted that the (R)-enantiomer of verapamil (score = −7.99) binds tighter than the (S)-enantiomer (score = −7.16); the former was employed as a second-generation Pgp MDR reversal agent.[1] Both verapamil (Fig. 2E) and tariquidar bound to the aromatic-rich pocket with site-1, which was the preferred binding site for the leuconicine base scaffold in a number of the top-ranking leuconicine A derivatives. To test the validity of our Pgp homology model, we selected the third highest docking hit **7** (score = −8.70), which is the 3,4,5-trimethoxybenzyl analogue of leuconicine A (**5**), and prepared it by synthesis (vide infra). The selected 3,4,5-trimethoxybenzyl analogue presented an additional interaction between the electron-rich arene group and an adjacent hydrophobic pocket formed by F343, I340, and L339 (Fig. 2).
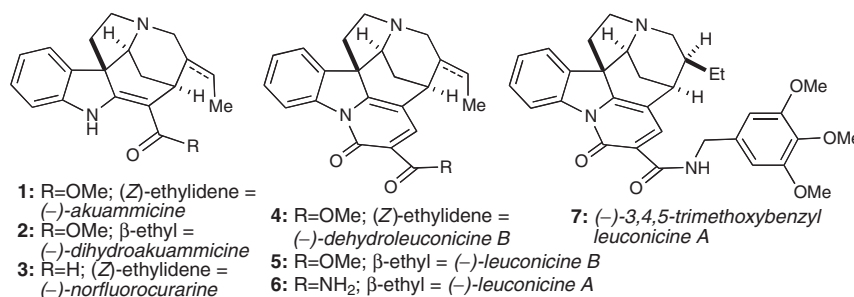

1: R=OMe; (Z)-ethylidene = (−)-akuammicine
2: R=OMe; β-ethyl = (−)-dihydroakuammicine
3: R=H; (Z)-ethylidene = (−)-norfluorocurarine

4: R=OMe; (Z)-ethylidene = (−)-dehydroleuconicine B
5: R=OMe; β-ethyl = (−)-leuconicine B
6: R=NH₂; β-ethyl = (−)-leuconicine A

7: (−)-3,4,5-trimethoxybenzyl leuconicine A

Figure 1. Structures of akuammicine (**1**), dihydroakuammicine (**2**), norfluorocurarine (**3**), dehydroleuconicine B (**4**), leuconicine B (**5**) and leuconicine A (**6**) and trimethoxybenzyl leuconicine A (**7**).
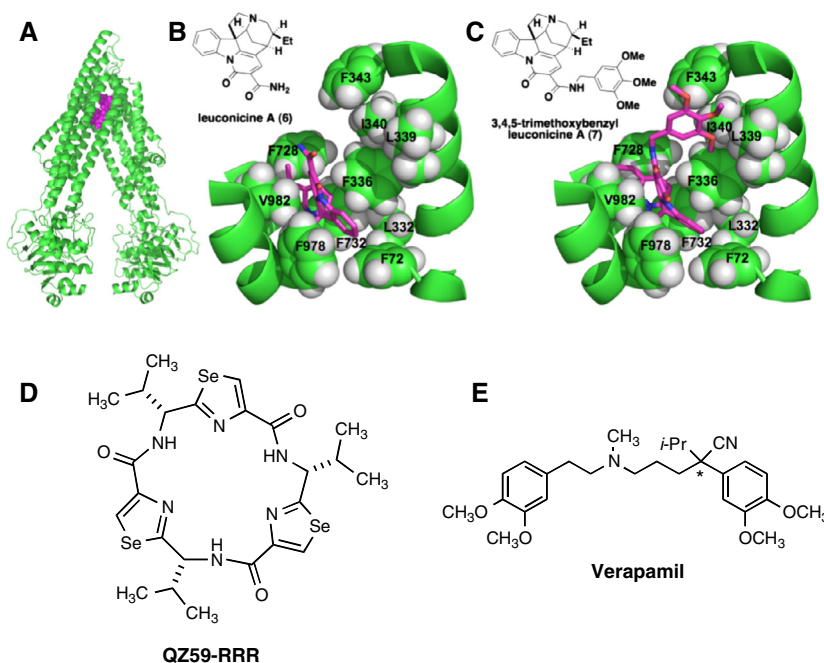
Figure 2. (A) Homology model of Pgp-glycoprotein (green) docked with leuconicine A (**6**, magenta); (B) structure of **6** and close-up view of **6** docked to Pgp homology model; (C) structure of 3,4,5-trimethoxybenzyl leuconicine A (**7**) and zoomed-in view of **7** docked to homology model; (D) structure of QZ59-RRR; and (E) structure of verapamil.

2.2. Chemistry

The syntheses of alkaloids **1**–**3** are outlined in Scheme 1. Employing the asymmetric method of Yus,[22] *N*-tosyl indole-3-car-boxaldehyde (**8**) was treated with (*R*)-*N*-*tert*-butane-sulfinylamine (**9**), Ti(OEt)$_4$, allylbromide and In(0) to furnish sulfinamide **10** in 87% yield (dr = 10:1). Removal of the auxiliary and *N*-tosyl group was accomplished by sequential treatment with 4 M HCl in dioxane followed by magnesium in MeOH to afford **11** in 75% yield

(one-pot). Alkylation with (*Z*)-2-iodobutenyl bromide[23] and acylation with bromoacetyl chloride furnished amide **12** in 83% yield (two steps).

Cross-metathesis of **12** and methyl acrylate employing 10 mol% of Hoveyda–Grubbs 2nd-generation (HG-II) catalyst[24] gave **13** in 80% yield. The key step was effected with AgOTf and 2,6-di-*t*-bu-tyl-4-methylpyridine (DTBMP) followed by DBU in toluene (dr = 13:1), delivering ABCE tetracycle **14** in 60% yield. Lactam reduction was realized with thionation with Lawesson's reagent
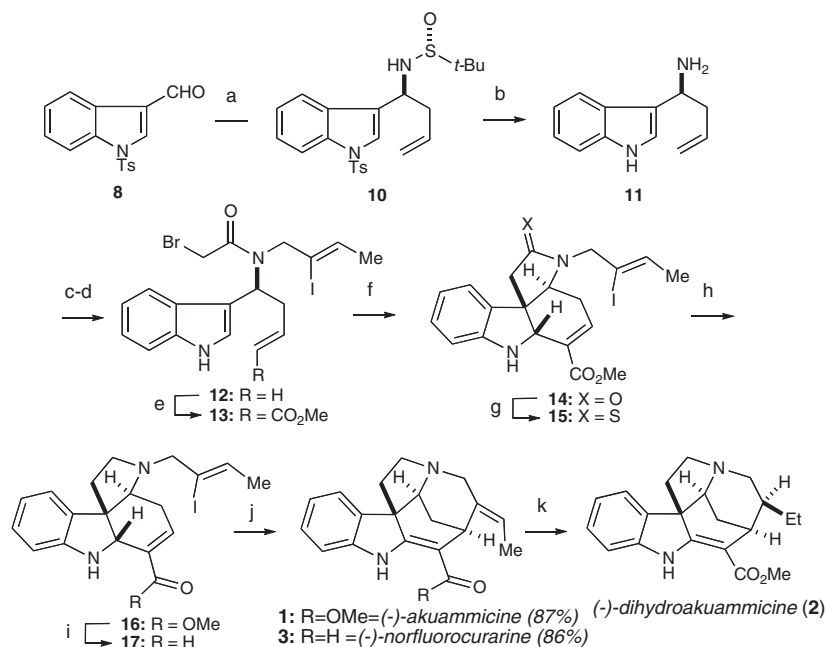
Scheme 1. Synthesis of Strychnos alkaloids **13**. Reagents and conditions: (a) (*R*)-*N*-*tert*-butanesulfinamide, Ti(OEt)$_4$ then allyl bromide, In(0), THF, 87% (dr = 10:1); (b) 4 M HCl in dioxane then Mg(0), MeOH, 75%; (c) Cs$_2$CO$_3$, (*Z*)-2-iodo-2-butenyl bromide; (d) BrAcCl, Et$_3$N, 83% over two steps; (e) methyl acrylate, 10 mol % Hoveyda–Grubbs 2nd-generation catalyst, CH$_2$Cl$_2$, 80%; (f) AgOTf, DTBMP then DBU, PhMe, 12 h, 60%; (g) Lawesson's reagent; (h) Et$_3$OBF$_4$ then NaBH$_4$ in MeOH, 80% over two steps; (i) LiNMe(OMe) then DIBAL-H, CH$_2$Cl$_2$, 89% over two steps; (j) Pd(OAc)$_2$, PPh$_3$, Et$_3$N; (k) PtO$_2$, H$_2$ (1 atm), MeOH, 85%.

to give **15** followed by Borch[25] reduction to afford **16** in 80% yield.[26] Rawal's intramolecular Heck reaction delivered (−)-akuammicine (**1**) in 87% yield.[27] To access (−)-norfluorocurarine (**3**), ester **16** was converted to aldehyde **17** using Weinreb's method.[28] Heck cyclization of **17** gave **3** in 86% yield. Finally, (−)-dihydroakuammicine (**2**) was prepared by hydrogenation of **1** with Adams's catalyst (85% yield).[29]

The syntheses of the leuconicines **5** and **6** are shown in Scheme 2. The pyridone ring in **19** was prepared in 82% yield by a novel one-pot sequential amidation-intramolecular Knovenagel condensation via **18**. Application of the Heck cyclization tactic delivered (−)-dehydroleuconicine B (**4**) in 81% yield. Chemoselective reduction of the ethylidene moiety was accomplished with Raney Ni in 82% yield. Weinreb aminolysis of **5** with dimethylaluminum amide[30] secured (−)-leuconicine A (**5**) in 91% yield.

As previously discussed, inspection of the Pgp homology model in Figure 2 indicated that the primary amide of leuconicine A (**6**) was proximal to a hydrophobic pocket formed by residues F343, I340, L339 and F336 (i.e., site 1). Docking studies revealed that analogue **7** was the third highest scoring hit, and its preparation could be realized from leuconicine A (**5**). To this end, we treated **5** with 3,4,5-trimethoxybenylamine and trimethylalane to afford leuconicine A analogue **7** in 79% yield.

2.3. In vitro binding assay

As MDR reversal agents act by binding and inhibiting Pgp, we quantified the affinity of alkaloids **1**−**7** for binding to purified Pgp. Specifically, we employed an established intrinsic tryptophan fluorescence quenching method to obtain K_d values.[31] The results are shown in Table 1. K_d values ranged from ∼100 μM for the low affinity compounds akauammicine (**1**) and its dihydro analogue **2** to 4.4 μM for 3,4,5-trimethoxybenzyl leuconcicine A (**7**), which had an affinity comparable to that of verapamil. The alkaloids fell into three groups: low affinity (80–100 μM for compounds **1**–**3**), medium affinity (14–16 μM for compounds **4**–**6**) and higher affinity for compound **7** and verapamil. Binding affinity correlated well with aromatic ring content and molecular weight (i.e., lipophilicity).[1]

Overall, the predicted binding poses of the tested compounds were highly similar, primarily interacting with the aforementioned aromatic-rich region of site-1 in Pgp. However unlike alkaloids **1**–**6**, both verapamil and 3,4,5-trimethoxybenzyl leuconicine A

Table 1
Affinity of synthetic alkaloids **1**–**7** and verapamil to purified Pgp, as determined by intrinsic tryptophan fluorescence quenching

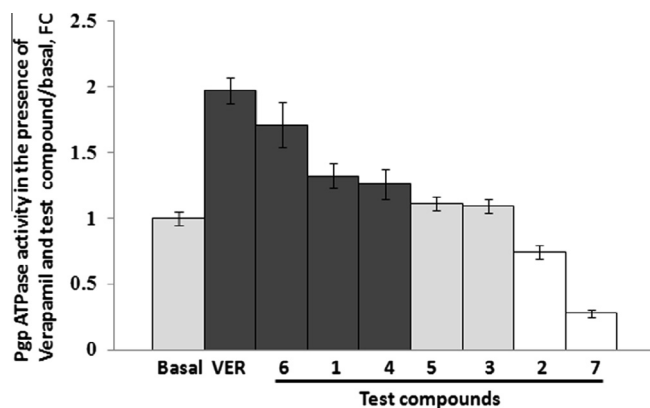| Test compound	ID	K_d (μM)
Akauammicine	**1**	99
Dihydroakuammicine	**2**	92
Norfluorocurarine	**3**	81
Dehydroleuconicine A	**4**	16.1
Leuconicine A	**5**	13.8
Leuconicine B	**6**	14.1
3,4,5-Trimethoxybenzyl leuconicine A	**7**	4.42
Verapamil	VER	2.40

Figure 3. The effect of compounds **1**–**7** (1 mM) on Pgp ATPase activity was assessed in the presence of recombinant human Pgp using Pgp-Glo assay system, as described in the experimental section. The results were normalized to basal activity in the absence of a test compound. Compound **7** had the strongest inhibitory effect on ATPase activity.

(**7**) interact with adjacent hydrophobic pockets in site-1 that likely contribute to their increased potency.

2.4. In vitro Pgp-associated ATPase assay

In parallel with binding experiments, we tested the effect of synthesized compounds **1**–**7** on Pgp ATPase activity associated with the transport function of Pgp using the Pgp-Glo assay. In this analysis, ATP is consumed by Pgp ATPase activity to promote transmembrane transport of the test compound. The remaining ATP is
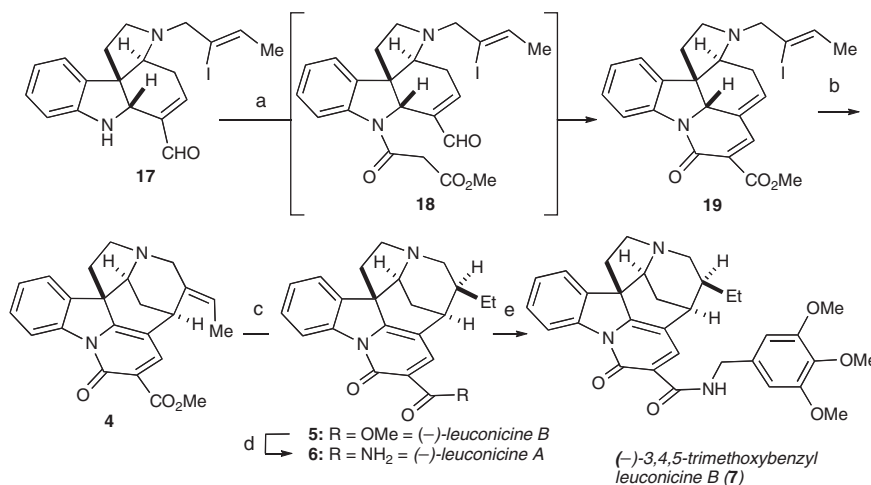
Scheme 2. Syntheses of leuconicines A (**6**), B (**5**) and 3,4,5-trimethoxybenzyl leuconicine A (**7**). Reagents and conditions: (a) methyl malonyl chloride, Et₃N, CH₂Cl₂, 82%; (b) Pd(OAc)₂, PPh₃, Et₃N, 81%; (c) Raney Ni, 82%; (d) NH₃, AlMe₃, 91%; (e) 3,4,5-trimethoxybenzylamine, AlMe₃, 79%.
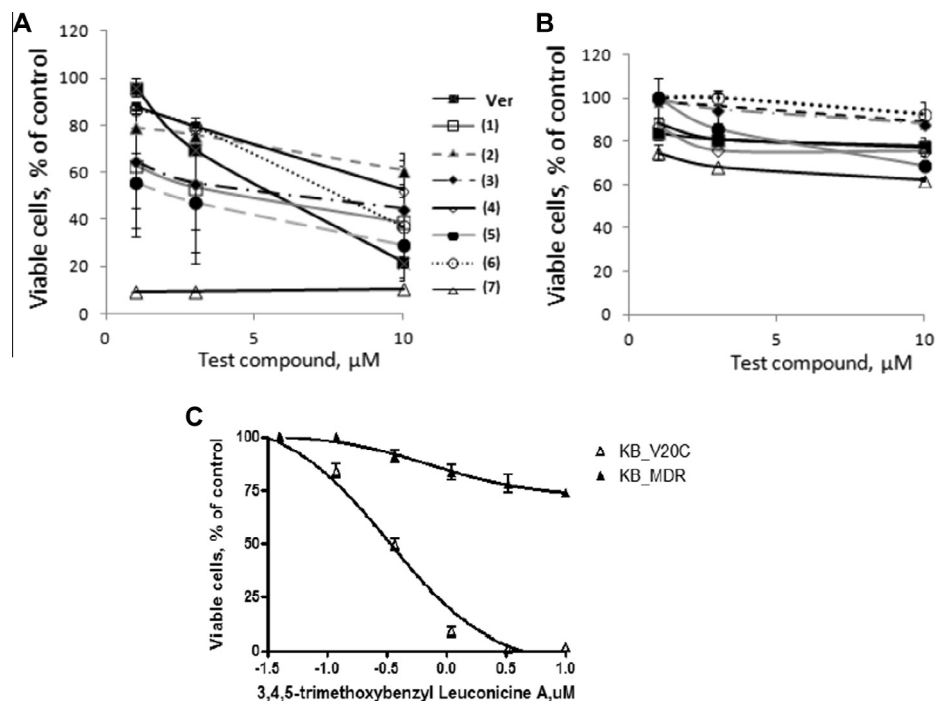
Figure 4. KB-V20C (Panel A) and KB-MDR (Panel B) cell growth in the presence of compounds **1**–**7**, or verapamil (Ver). Panel C shows cytotoxic effect of 3,4,5-trimethoxybenzyl Leuconicine (**7**) in KB-V20C (△) and KB-MDR (▲) cell lines.

then detected by luciferase-generated luminescence signal. The assay provides a rapid method to detect inhibitory or stimulatory effects of test compounds at high concentrations (1 mM). Figure 3 summarizes the changes in Pgp ATPase activity in the presence of verapamil and test compounds **1**–**7** normalized to basal activity. As shown in Figure 3, test compounds manifest weak (**1**, **3**, **4**, **5**) to moderate (**6**) stimulatory effects similar to that of verapamil, while compounds **2** and **7** had an inhibitory effect on ATPase activity. The Pgp-Glo in vitro assay helped to perform the fast preliminary screen of synthesized compounds and correctly identified compound **7** as a promising strong inhibitor of Pgp-associated ATPase activity.

2.5. MDR reversal activity in drug-resistant tumor cell lines

Finally, we estimated cytotoxic/cytostatic effects, and the reversal effect of test compounds on the sensitivity of MDR cell lines to the anticancer drugs vincristine and doxorubicin. To

establish the pharmacological characteristics of test compounds, their cytostatic/cytotoxic effects were first evaluated by the MTT (3-(4,5-dimethylthiazol-2-yl)-2,5-diphenyltetrazolium bromide) assay in two cancer cell lines overexpressing Pgp.[32] Incubation of KB-MDR or KB-V20C cells with test compounds **1**–**7** resulted in a concentration-dependent decrease of viable cells (Fig. 4A and B). Importantly, KB-MDR was more resistant to all tested compounds than KB-V20C. Compound **7** had the highest cytotoxic effect on KB-V20C cells (IC_{50} = 0.38 ± 0.032 μM, Fig. 4C). Therefore, in all subsequent MDR reversal experiments we used compounds **1**–**7** at concentration that resulted in no more than a 50% decrease of viable cells after a four day incubation: 1–3 μM for test compounds **1**–**6**, and 0.07–1.0 μM for compound **7**.

To estimate the MDR reversal effect of alkaloids **1**–**7** on the sensitivity of Pgp-overexpressing cells KB-V20C or KB-MDR to vincristine and doxorubicin, we treated cells with alkaloids **1**–**7** at final concentrations 0.07–3.0 μM for 1 h. Treatment with 1 μM verapamil was used as a positive control, and the negative control
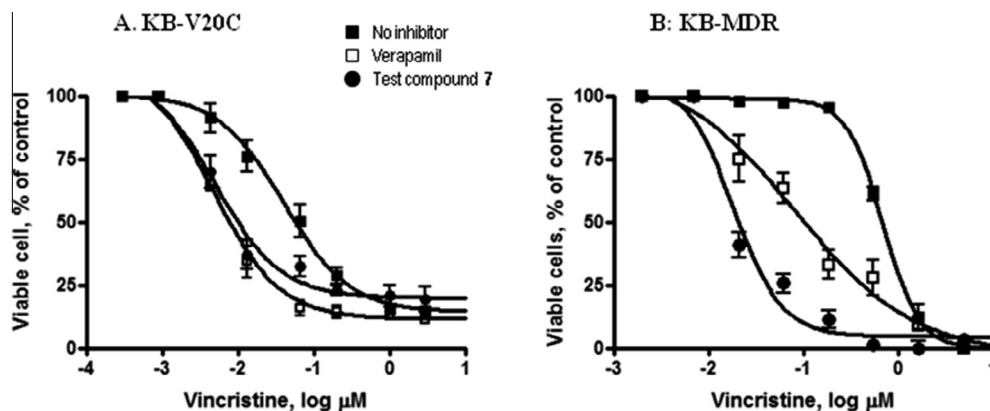

Figure 5. Reversal of sensitivity to vincristine in the presence of compound **7**. Verapamil was used as positive control. Panel A: KB-V20C, 1 μM verapamil, and 70 nM compound **7**. Panel B: KB-MDR, 10 μM verapamil, and 1 μM compound **7**.

Table 2
Cytotoxicity (IC$_{50}$) of vincristine in KB-V20C and KB-MDR cell lines[*] over-expressing Pgp in the presence of compounds **1–7**

Test compound	ID	Test compound, (µM)	Vincristine, IC$_{50}$, (µM)		IC$_{50}$, Fold change, VER/test compound	
			KB-V20C	KB-MDR	KB-V20C	KB-MDR
No inhibitor		0	0.05 ± 0.021	1 ± 0.41		
Verapamil	VER	1	0.003 ± 0.0014	1.5 ± 0.63	1.0	1.0
Akuammicine	1	1	0.02 ± 0.005	0.6 ± 0.03	0.2	2.5
		3	0.007 ± 0.0012	0.4 ± 0.03	0.4	3.8
Dihydroakuammicine	2	1	0.04 ± 0.011	0.6 ± 0.03	0.1	2.5
		3	0.017 ± 0.005	0.4 ± 0.05	0.2	3.8
Norfluorocurarine	3	1	0.02 ± 0.008	0.7 ± 0.11	0.2	2.1
		3	0.01 ± 0.005	0.7 ± 0.06	0.3	2.1
19,20-Dehydro-	4	1	0.02 ± 0.002	0.7 ± 0.03	0.2	2.1
Leuconicine B		3	0.01 ± 0.004	0.4 ± 0.05	0.3	3.8
Leuconicine B	5	1	0.02 ± 0.002	0.4 ± 0.05	0.2	3.8
		3	0.01 ± 0.001	0.22 ± 0.01	0.3	6.8
Leuconicine A	6	1	0.012 ± 0.004	0.4 ± 0.03	0.3	3.8
		3	0.005 ± 0.001	0.3 ± 0.01	0.6	5.0
3,4,5-		0.07	0.005 ± 0.001	0.7 ± 0.16	0.6	2.1
Trimethoxybenzyl	7	0.14	0.003 ± 0.001	0.6 ± 0.07	1.0	2.5
Leuconicine A		0.28	0.002 ± 0.001	0.4 ± 0.05	1.5	3.8
		1	Toxic	0.016 ± 0.005	n/a	93.8

[*] Parental cell line KB is highly sensitive to vincristine: IC$_{50}$ = 0.003 µM.

contained no inhibitors. Next, 3-fold serial dilutions of doxorubicin, or vincristine were added to the cells. After a four-day incubation, cell viability was determined by MTT assay. The IC$_{50}$ values for vincristine and doxorubicin were calculated by fitting the sigmoid E_{max} model to a plot of cell viability versus drug concentration (Fig. 5).

Table 2 summarizes the results of MDR reversal experiments in two cell lines incubated with serial dilutions of vincristine in the absence of Pgp inhibitor, in the presence of verapamil (positive control), or different concentrations of compounds **1–7**.

Importantly, compound **7** at a concentration of 70 nM increased the sensitivity of KB-V20C cells to vincristine by an order of magnitude, and at 1 µM concentration, it increased the sensitivity of KB-MDR cells to vincristine about 60-fold. At 1 µM concentration, compound **7** was approximately 90 times more potent as a MDR reversal agent by 'sensitivity index' (ratio of IC$_{50}$ for verapamil to that of compound **7**, as shown in the Table 2, right column). Similarly, in the presence of compound **7** at 1 µM, the sensitivity of KB-MDR cells to doxorubicin increased about 20-fold (IC$_{50}$ = 5.7 ± 2.35 µM vs 0.3 ± 0.13 µM). Interestingly, verapamil and compound **7** demonstrated similar Pgp affinity (K_d of 2.4 and 4.4 µM, respectively, Table 1). The distinct effects of verapamil and compound **7** on Pgp-mediated MDR suggest that their Pgp binding could invoke different molecular events. We speculate that while verapamil is a competitive inhibitor of Pgp, compound **7** is possibly an allosteric regulator of Pgp transport activity. This hypothesis needs further experimental investigation.

3. Conclusion

We have employed a highly efficient and effective synthetic route to prepare *Strychnos* alkaloids and their derivatives thereof and employed docking studies to design an analogue with enhanced potency compared to prototype molecules. Results of in vitro and cell-based assays identified 3,4,5-trimethoxybenzyl leuconicine B (**7**) as a potent Pgp inhibitor and MDR reversal agent. At a concentration of 70 nM, this compound increased sensitivity of Pgp-expressing KB-V20C cells to vincristine around 10-fold, and at 1 µM it increased sensitivity of Pgp-expressing KB-MDR cells to doxorubicin about 90-fold. Our data on MDR reversal in the human cancer cells overexpressing Pgp suggest that the potential of compound **7** as a strong inhibitor of vincristine efflux from tumor cells needs to be further investigated. Compound **7** will be

used as a lead to further optimize the Pgp inhibitory activity/cytotoxicity of the *Strychnos* scaffold.

4. Experimental section

4.1. Chemistry

4.1.1. General

All reactions containing water or air sensitive reagents were performed in oven-dried glassware under nitrogen or argon. Tetrahydrofuran and dichloromethane were passed through two columns of neutral alumina. Toluene was passed through one column of neutral alumina and one column of Q5 reactant. Triethylamine was distilled from CaH$_2$ prior to use, and 4 Å molecular sieves were activated by flame-drying under vacuum. AgOTf was azeotroped with dry toluene prior to use. Compounds **4–6** and **10–17** were prepared according to the procedures of Andrade.[9] (Z)-2-Iodobutenyl bromide was prepared according to the procedure of Rawal.[19] All other reagents were purchased from commercial sources and used without further purification. All solvents for work-up procedures were used as received. Flash column chromatography was performed with ICN Silitech 32–63 D 60 Å silica gel with the indicated solvents. Thin layer chromatography was performed on Analtech 60F$_{254}$ silica gel plates. Detection was performed using UV light, KMnO$_4$ stain, PMA stain and subsequent heating. ^{1}H and ^{13}C NMR spectra were recorded at the indicated field strength in CDCl$_3$ at rt. The purity of each tested compounds (>95%) was determined on an Agilent 1200 LC/MS instrument using a Kinetex 2.6u C18 column (30 × 2.1 mm, with a flow rate of 1 mL/min and detection at 254 nm) employing a 5–100% acetonitrile/water/0.1% formic acid gradient.

4.1.2. (−)-Akuammicine (1)

Palladium(II) acetate (7.0 mg, 0.0313 mmol) and PPh$_3$ (16.4 mg, 0.0626 mmol) were added to a solution of **16** (47 mg, 0.1044 mmol) in Et$_3$N (5 mL). The reaction mixture was purged with Argon for 10 min, heated to 90 °C (oil bath) and stirred for 3.5 h. After cooling to rt, the mixture was diluted with CH$_2$Cl$_2$ (25 mL), washed with brine (10 mL), dried (Na$_2$SO$_4$) and filtered. The solvent was concentrated under reduced pressure, and the residue was purified by flash column chromatography eluting with MeOH/CH$_2$Cl$_2$ (0.4:9.6 → 1:9). The material was washed with a solution of 25% aq NaOH (10 mL), which afforded 24 mg (71%) of

1 as white solid whose NMR spectra (^{1}H and ^{13}C) were identical with reported literature values.[33] The optical rotation for synthetic material was: $[\alpha]_D^{20}$ −769 (c 0.4, CHCl$_3$) whereas the literature value was: $[\alpha]_D^{20}$ −737 (c 0.5, CHCl$_3$).[34]

4.1.3. (−)-Norfluorocurarine (2)

Palladium(II) acetate (24.1 mg, 0.107 mmol) and PPh$_3$ (56.2 mg, 0.214 mmol) were added to a solution of **17** (150 mg, 0.357 mmol) in Et$_3$N (18 mL). The reaction mixture was purged with Argon for 20 min, heated to 90 °C (oil bath) and stirred for 3.0 h. After cooling to rt, the mixture was diluted with CH$_2$Cl$_2$ (25 mL), washed with brine (10 mL), dried (Na$_2$SO$_4$) and filtered. The solvent was concentrated under reduced pressure, and the residue was purified by flash column chromatography eluting with MeOH/CH$_2$Cl$_2$ (0.4:9.6 → 1:9). The material was washed with a solution of 25% aq NaOH (10 mL), which afforded 90 mg (86%) of **2** as yellow liquid whose NMR spectra (^{1}H and ^{13}C) were identical with reported literature values.[35] The optical rotation for synthetic material was: $[\alpha]_D^{20}$ −1184 (c 0.5, CHCl$_3$) whereas the literature value was: $[\alpha]_D^{20}$ −1230 (c 0.5, CHCl$_3$).[31]

4.1.4. (−)-19,20-Dihydroakuammicine (3)

Excess PtO$_2$ (10 mg) was added to a solution of (−)-akuammicine (**1**) (11 mg, 0.0341 mmol) in CH$_3$OH (4 mL). The reaction mixture was stirred for 12 h under a H$_2$ atmosphere, filtered through a short bed of Celite (pre-wet with CH$_3$OH) and the solvent was evaporated under reduced pressure. The residue was purified by flash column chromatography eluting with MeOH/CH$_2$Cl$_2$ (0.5:9.5), to give 10.5 mg (95%) of **3** as light yellowish oil whose NMR spectra

(^{1}H and ^{13}C) were identical with reported literature values.[36] The optical rotation for synthetic material was: $[\alpha]_D^{20}$ −508 (c 0.55, CH$_3$OH) whereas the literature value was: $[\alpha]_D^{20}$ −568 (c 0.175, CH$_3$OH).[32]

4.1.5. (−)-3,4,5-Trimethoxybenzyl leuconicine A (7)

To a stirred solution of Me$_3$Al (0.31 mL, 2 M in toluene, 0.63 mmol) in CH$_2$Cl$_2$ (3 mL) at −15 °C was added 3,4,5-trimethoxybenzyl amine (93 μL 0.55 mmol). The reaction mixture was stirred for 20 min then warmed to rt. Stirring was continued for an additional 1 h. (−)-Leuconicine B (**5**) (40 mg, 0.11 mmol) dissolved in CH$_2$Cl$_2$ (2 mL) was added, and the reaction mixture was refluxed for overnight. After cooling to rt, the reaction was quenched with aq 1 N HCl (2 mL), stirred for 30 min, and extracted with CHCl$_3$ (3 × 10 mL). The combined organic layers were washed with brine (1 × 10 mL), and dried over Na$_2$SO$_4$. The solvent was concentrated under reduced pressure, and the residue was purified by flash column chromatography eluting with MeOH/CH$_2$Cl$_2$ (1.0:9.0) to give 42 mg (79%) of **7**. $[\alpha]_D^{25}$ −424 (c 0.9, CHCl$_3$); IR (neat) 3760, 3010, 2980, 1760, 1691, 1100, 730 cm^{-1}; ^{1}H NMR (400 MHz) δ 10.07 (t, J = 5.6 Hz, 1H), 8.41 (dd, J = 8, 0.8 Hz, 1H), 8.25 (s, 1H), 7.39–7.33 (m, 2H), 7.29 (dd, J = 7.6, 1.2 Hz, 1H), 6.61 (s, 2H), 4.60 (t, J = 6.6Hz, 2H), 4.02 (t, J = 2.4 Hz, 1H), 3.80 (s, 6H), 3.75 (s, 3H), 3.11–3.08 (m, 1H), 2.95 (dd, J = 6.2, 3.2 Hz, 1H), 2.86–2.79 (m, 3H), 2.13 (dt, J = 12.4, 2.8 Hz, 1H), 1.94–1.80 (m, 3H), 1.44–1.40 (m, 1H), 1.30 (dt, J = 13.6, 3.2 Hz, 1H), 1.25–1.18 (m, 1H), 0.99 (t, J = 7.4 Hz, 3H); ^{13}C NMR (100 MHz) δ 164.3, 162.0, 160.7, 153.6, 145.2, 140.9, 140.3, 134.8, 128.4, 127.3, 120.6, 120.5, 117.7, 116.2, 105.0, 77.9, 62.5, 61.0, 56.3, 55.8, 54.7, 51.8, 45.2, 44.0, 39.0, 36.5, 31.6, 29.9, 26.7, 11.7; HRMS(FAB) calc'd for C$_{32}$H$_{35}$N$_3$O$_5$+H = 542.2655, found 542.0376.

4.2. General procedure for in vitro binding assay

To obtain K_d values, an established intrinsic tryptophan fluorescence quenching method was used as described elsewhere.[27]

4.3. General procedure for in vitro Pgp-associated ATPase assay

The inhibitory or stimulatory effect of a test compound on ATPase activity of human recombinant Pgp was assessed in vitro using the Pgp-Glo Assay System (Promega, WI). Briefly, recombinant human Pgp membranes were incubated with ATP in the presence of 0.3 mM sodium vanadate (an ATPase inhibitor), 0.5 mM verapamil (and ATPase stimulator), or 0.3–1 mM of the test compounds. The reaction was initiated by adding ATP to a final concentration 5 mM. After 40 min incubation at 37 °C, the reaction was stopped by addition of ATP detection reagent, and the amount of residual ATP was estimated by measuring luciferase-generated bioluminescence. All reactions were replicated three times, in two independent experiments. The difference in sample luminescence was used to calculate the effect of a test compound on Pgp ATPase activity.

4.4. General procedure for MDR reversal assay

Growth inhibition assays were performed in three cell lines, the parental human oral epidemoid carcinoma KB cells, and two lines (KB-MDR and KB-V20C) overexpressing Pgp. KB-MDR was generated by infection of KB with a retroviral vector carrying the human mdr-1 gene, and was grown in the presence of 37 nM doxorubicin. KB-V20C cell line was developed from the parental KB cells by stepwise selection for resistance with increasing concentrations of vincristine (VCR), and was grown in the presence of 20 nM VCR. All three cell lines were a generous gift from Dr. Yung-Chi Cheng (Yale University School of Medicine) and were maintained in RPMI1640 medium supplemented with 10% FBS, antibiotic/antimycotic, and cytotoxic drug (DOX or VCR) where indicated. Cell growth and viability were measured by flow cytometry with Guava Personal Cell Analyzer (PCA, Guava Technologies, Hayward, CA) using ViaCount reagent (Millipore, Hayward, CA), as described earlier.[37] Cells were seeded in 96-well plate at 1000 cells (KB-MDR) or 2000 cells (KB-V20C) per well and treated with test compounds at concentrations 1, 3, 10 μM for four days. For the MTT (3-(4,5-dimethylthiazol-2-yl)-2,5-diphenyltetrazolium) assay (CellTiter 96 cell proliferation kit, Promega, WI), cells (1000–2000 cells per well) were plated into 96-well plates, and cultured for 4 days in varying concentrations of the test compounds. After incubation, MTT reagent was added to each well, and endpoint data collected by a SpectraMax M2 microplate spectrophotometer (Molecular Device, CA) according to the manufacturer's instructions. The IC$_{50}$ values were calculated using GraphPad Prism (GraphPad Software Inc., CA) by fitting a sigmoid E_{max} model to the cell viability versus drug concentration data, as determined in duplicate from three independent experiments.

5. Disclaimer

The opinions, findings, conclusions, or other recommendations expressed herein are the private views of the authors and do not necessarily reflect the views of the U.S. Department of Defense or the U.S. Defense Threat Reduction Agency. This paper has been approved for public release with unlimited distribution.

the Defense Threat Reduction Agency through projects TMTI0 004.09.BH.T (AW, recipient).

Supplementary data

Supplementary data (^{1}H and ^{13}C NMR spectra of **1**, **2**, **3**, and **7**) associated with this article can be found, in the online version, at http://dx.doi.org/10.1016/j.bmc.2013.12.022.

References and notes

1. Eckford, P. D. W.; Sharom, F. J. *Chem. Rev.* **2009**, *109*, 2989.
2. Gottesman, M. M.; Fojo, T.; Bates, S. E. *Nat. Rev. Cancer* **2002**, *2*, 48.
3. Tsuruo, T.; Iida, H.; Tsukagoshi, S.; Sakurai, Y. *Cancer Res.* **1981**, *41*, 1967.
4. Futscher, B. W.; Foley, N. E.; GleasonGuzman, M. C.; Meltzer, P. S.; Sullivan, D. M.; Dalton, D. S. *Int. J. Cancer* **1996**, *66*, 520.
5. Palmeira, A.; Sousa, E.; Vasconcelos, M. H.; Pinto, M. M. *Curr. Med. Chem.* **2012**, *19*, 1946.
6. Szakács, G.; Paterson, J. K.; Ludwig, J. A.; Booth-Genthe, C.; Gottesman, M. M. *Nat. Rev. Drug Disc.* **2006**, *5*, 219.
7. List, A. F.; Kopecky, K. J.; Head, D. R.; Persons, D. L.; Slovak, M. L.; Dorr, R.; Karanes, C.; Hynes, H. E.; Doroshow, J. H.; Shurafa, M.; Appelbaum, F. R. *Blood* **2001**, *98*, 3212.
8. Wattel, E.; Solary, E.; Hecquet, B.; Caillot, D.; Ifrah, N.; Brion, A.; Milpied, N.; Janvier, M.; Guerci, A.; Rochant, H.; Cordonnier, C.; Dreyfus, F.; Veil, A.; Hoang-Ngoc, L.; Stoppa, A. M.; Gratecos, N.; Sadoun, A.; Tilly, H.; Brice, P.; Lioure, B.; Desablens, B.; Pignon, B.; Abgrall, J. P.; Leporrier, M.; Dupriez, B.; Guyotat, D.; Lepelley, P.; Fenaux, P. *Adv. Exp. Med. Biol.* **1999**, *457*, 35.
9. Tamaki, A.; Ierano, C.; Szakács, G.; Robey, R. W.; Bates, S. E. *Essays Biochem.* **2011**, *50*, 209.
10. Cragg, G. M.; Grothaus, P. G.; Newman, D. J. *Chem. Rev.* **2009**, *109*, 3012.
11. Gan, C.-Y.; Low, Y.-Y.; Etoh, T.; Hayashi, M.; Komiyama, K.; Kam, T.-S. *J. Nat. Prod.* **2009**, *72*, 2098.
12. Sirasani, G.; Andrade, R. B. *Org. Lett.* **2009**, *11*, 2085.
13. Sirasani, G.; Andrade, R. B. *Org. Lett.* **2011**, *13*, 4736.
14. Woodland, C.; Koren, G.; Wainer, I. W.; Batist, G.; Ito, S. *Can. J. Physiol. Pharmacol.* **2003**, *81*, 800.
15. Pearce, H. L.; Safa, A. R.; Bach, N. J.; Winter, M. A.; Cirtain, M. C.; Beck, W. T. *Proc. Natl. Acad. Sci.* **1989**, *86*, 5128.
16. Berman, H. M.; Westbrook, J.; Feng, Z.; Gilliland, G.; Bhat, T. N.; Weissig, H.; Shindyalov, I. N.; Bourne, P. E. *Nucleic Acids Res.* **2000**, *28*, 235.
17. Aller, S. G.; Yu, J.; Ward, A.; Weng, Y.; Chittaboina, S.; Zhuo, R.; Harrell, P. M.; Trinh, Y. T.; Zhang, Q.; Urbatsch, I. L.; Chang, G. *Science* **2009**, *323*, 1718.
18. Jacobson, M. P.; Pincus, D. L.; Rapp, C. S.; Day, T. J.; Honig, B.; Shaw, D. E.; Friesner, R. A. *Proteins* **2004**, *55*, 351.
19. Friesner, R. A.; Banks, J. L.; Murphy, R. B.; Halgren, T. A.; Klicic, J. J.; Mainz, D. T.; Repasky, M. P.; Knoll, E. H.; Shelley, M.; Perry, J. K.; Shaw, D. E.; Francis, P.; Shenkin, P. S. *J. Med. Chem.* **2004**, *47*, 1739.
20. Halgren, T. A.; Murphy, R. B.; Friesner, R. A.; Beard, H. S.; Frye, L. L.; Pollard, W. T.; Banks, J. L. *J. Med. Chem.* **2004**, *47*, 1750.
21. Ding, P. R.; Tiwari, A. K.; Ohnuma, S.; Lee, J. W.; An, X.; Dai, C. L.; Lu, Q. S.; Singh, S.; Yang, D. H.; Talele, T. T.; Ambudkar, S. V.; Chen, Z. S. *PLoS ONE* **2011**, *6*, e19329.
22. Gonzalez-Gomez, J. C.; Medjahdi, M.; Foubelo, F.; Yus, M. *J. Org. Chem.* **2010**, *75*, 6308.
23. Rawal, V. H.; Michoud, C. *J. Org. Chem.* **1993**, *58*, 5583.
24. Garber, S. B.; Kingsbury, J. S.; Gray, B. L.; Hoveyda, A. H. *J. Am. Chem. Soc.* **2000**, *122*, 8168.
25. Borch, R. F. *Tetrahedron Lett.* **1968**, *9*, 61.
26. Raucher, S.; Klein, P. *Tetrahedron Lett.* **1984**, *21*, 4061.
27. Rawal, V. H.; Michoud, C. *Tetrahedron Lett.* **1991**, *32*, 1695.
28. Nahm, S.; Weinreb, S. M. *Tetrahedron Lett.* **1981**, *22*, 3815.
29. Bonjoch, J.; Solé, D.; García-Rubio, S.; Bosch, J. *J. Am. Chem. Soc.* **1997**, *119*, 7230.
30. Basha, A.; Lipton, M.; Weinreb, S. M. *Tetrahedron Lett.* **1977**, *18*, 4171.
31. Liu, R.; Siemiarczuk, A.; Sharom, F. J. *Biochemistry* **2000**, *9*, 14927.
32. Burton, J. A. Methods in Molecular Medicine Vol. 110: Chemosensitivity: Vol. 1. In *In Vitro Assays*; Blumenthal, R. D., Ed.; Humana Press: Totowa NJ, 2005; pp 69–78.
33. Jones, S. B.; Simmons, B.; Mastracchio, A.; MacMillan, D. W. C. *Nature* **2011**, *475*, 183.
34. Henry, A. T.; Sharp, M. T. *J. Chem. Soc.* **1927**, 1950.
35. Stauffacher, D. *Helv. Chim. Acta* **1961**, *44*, 2006.
36. Amat, M.; Coll, M. D.; Bosch, J.; Espinosa, E.; Molins, E. *Tetrahedron: Asymmetry* **1997**, *8*, 935.
37. Phadke, M.; Krynetskaia, N.; Krynetskiy, E. *Anticancer Drugs* **2013**, *24*, 366–374.